Proteomic alteration of PK-15 cells after infection by porcine circovirus type 2

Jie Liu · Juan Bai · Lili Zhang · Chengcai Hou ·
Yufeng Li · Ping Jiang

Abstract Porcine circovirus type 2 (PCV2) has been identified as the essential causal agent of post-weaning multisystemic wasting syndrome, which has spread worldwide. To discover cellular protein responses of PK-15 cells to PCV2 infection, two-dimensional liquid chromatography–tandem mass spectrometry (MS) coupled with isobaric tags for relative and absolute quantification (iTRAQ) labeling was employed to quantitatively identify the proteins that were differentially expressed in PK-15 from the PCV2-infected group compared to the uninfected control group. A total of 196 cellular proteins in PK-15 that were significantly altered at different time periods post-infection were identified. These differentially expressed proteins were related to the biological processes of binding, cell structure, signal transduction, cell adhesion, etc. and their interactions. Moreover, some of these proteins were further confirmed by Western blot. The high number of differentially expressed proteins identified should be very useful in elucidating the mechanism of replication and pathogenesis of PCV2 in the future.

Keywords Porcine circovirus type 2 · PK-15 cells · Cellular proteins · iTRAQ

J. Liu · J. Bai · L. Zhang · C. Hou · Y. Li · P. Jiang (✉)
Key Laboratory of Animal Diseases Diagnostic and Immunology, Ministry of Agriculture, College of Veterinary Medicine, Nanjing Agricultural University, Nanjing 210095, People's Republic of China
e-mail: jiangp@njau.edu.cn

P. Jiang
Jiangsu Co-innovation Center for Prevention and Control of Important Animal Infectious Diseases and Zoonoses, Yangzhou, China

Introduction

Porcine circovirus type 2 (PCV2) is an immunosuppressive virus in pigs. It is a small, nonenveloped, single-stranded DNA virus that belongs to the circoviridae family [1]. The virus genome contains two major open reading frames (ORFs), ORF1 and ORF2. ORF1 encodes the replication proteins which are involved in virus replication, and ORF2 encodes the capsid (Cap) protein [2, 3]. PCV2 has been identified as the etiologic agent of the Postweaning Multisystemic Wasting Syndrome (PMWS) [4, 5] that is widely spread in swine farms and represents one of several porcine circovirus associated diseases (PCVAD). PCV2 infection usually accompanies lymphocyte or monocyte depletion and thus further results in immune suppression in the disease [6, 7]. The immunosuppressive disease mainly presents as PMWS, which caused a great economic loss worldwide [8, 9]. However, the immunosuppressive and pathogenic mechanisms have remained unclear in PCV2-infected pigs.

Proteomics analysis is a powerful technology used in a myriad of studies, including those focused on infectious diseases [10, 11]. Isobaric tags for relative and absolute quantification (iTRAQ) combined with multidimensional liquid chromatography (LC) and tandem MS analysis are emerging as a powerful methodology in the search for disease-specific targets [12, 13]. The iTRAQ reagent labels the primary amines on the peptides and thus can theoretically allow the tagging of most tryptic peptides. The multiplexing ability afforded by the iTRAQ reagents, which are available in four to eight different tags, suited the design of our present study.

Although PCVAD causes substantial economic losses, PCV2 pathogenesis is not fully understood. For elucidation of the interaction between host and PCV2, proteome

analysis has been utilized for host cellular responses to virus infection. Ramírez-Boo [14] used two proteomics strategies, 2-DE and 1-DE, followed by (16)O/(18)O peptide labeling, identification, and quantification via MS, leading to the detection of more than 100 differentially expressed proteins during PCV2 infection in an in vivo environment. Additionally, Zhang et al. [15] identified 34 host-encoded proteins that were altered in PCV2-infected PK-15 cells using two-dimensional gel electrophoresis (2-DE) coupled with MALDI-TOF/TOF, while Fan and colleagues [16] detected 163 proteins that were significantly affected in PCV2-infected PK-15 cells with the SI-LAC-based approach. The group of Cheng [17] examined PCV2-infected porcine alveolar macrophages (PAMs) using 2-DE, followed by MALDI-TOF/TOF, and identified 21 host-encoded proteins modified by the virus. A quantitative proteomics approach by our group revealed significant alterations in 145 cellular proteins in PCV2 infected PAMs at different time periods post-infection [18].

In the current study, we described quantitative proteomic analysis of a highly permissive PK-15 cell line (cloned by our laboratory) infected with PCV2 using isobaric tags for relative and absolute quantification, combined with multidimensional liquid chromatography and tandem MS analysis. Overall, we detected 196 proteins showing significant alterations in expression at different time periods post-infection. These proteins may serve as potential biomarkers to establish the interactions between PK-15 and PCV2, and provide novel insights into the mechanisms of disease onset.

Materials and methods

Reagents

Tris-base, SDS, and the 2-D Quantification Kit were purchased from GE Healthcare (Piscataway, NJ, USA). Octane and sequencing grade-modified trypsin were obtained from Sigma-Aldrich (St. Louis, MO). The iTRAQ Reagent Kit was acquired from Applied Biosystems (Foster City, CA). Acetonitrile (ACN) was purchased from Fisher Scientific (Pittsburgh, PA), formic acid (FA) from TEDIA (Fairfield, OH), and trichloroacetic acid (TCA), KH_2PO_4, methanol, acetone, HCl, and KCl from Sinopharm Chemical Reagent Co., Ltd. (Shanghai, China). All buffers were prepared with Milli-Q water (Millipore; Billerica, MA).

Cell culture and virus infection

Porcine circovirus type 2 strain, WG09 (GenBank accession no. GQ845027), was isolated from an intensive pig farm in Shanghai, China, in 2009. The virus stock was a fourth-passage cell culture prepared in PK-15 cells with a titer of $10^{6.0}$ $TCID_{50}$/mL. PK-15 cells were grown in Dulbecco's Modified Eagle's Medium supplemented with 10 % fetal bovine serum (GIBCO, Invitrogen Corporation, CA). Cells were seeded in 25-cm^2 culture flasks (Costar, Corning Incorporated, NY) until 75 % confluence. Next, cells were inoculated with PCV2 WG09 strain at 1 MOI and collected at 12, 24, 48, and 96 h post-inoculation (hpi), respectively. The amount of fetal bovine serum in medium was decreased to 2 %. Uninfected cells served as the mock infection group (Fig. 1). Viral propagation was confirmed via the indirect immunofluorescence assay and Western blot using a monoclonal antibody against PCV2 Cap protein (made in our laboratory).

Protein isolation, digestion, and labeling with iTRAQ reagents

After culture supernatant was being removed, cells were collected using a cell scraper after the addition of 300 µL lysis buffer (7 M urea, 2 M thiourea, 2 % (w/v) CHAPS) containing a complete protease inhibitor cocktail to the flask. Cells were lysed by sonication, the soluble protein fraction harvested by centrifugation at 15,000 × g for 40 min at 4 °C, and the pellet discarded. The protein concentration in the supernatant was determined using the 2-D Quant Kit (GE Healthcare, Piscataway, NJ). Protein (100 µg) from PK-15 cells was precipitated with acetone overnight at -20 °C and dissolved using iTRAQ dissolution buffer. After reduction and alkylation, protein solutions were digested overnight at 37 °C with sequence grade-modified trypsin (Promega) and labeled with iTRAQ tags, as described in the iTRAQ protocol (Applied Biosystems).
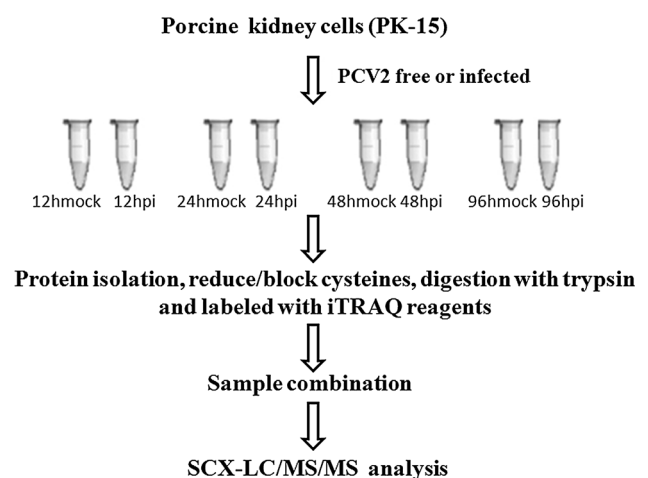

Fig. 1 Strategy for isobaric tags for relative and absolute quantification (iTRAQ)-coupled two-dimensional liquid chromatography–tandem mass spectrometry (2D LC–MS/MS) analysis of PK-15 cells infected with PCV2

Labeled digests were mixed and dried using a rotary vacuum concentrator (Christ RVC 2-25; Osterode am Harz, Germany). Two independent biological replicates were prepared and analyzed using iTRAQ-based LC–MS/MS.

Off-line 2D LC–MS/MS

The combined peptide mixtures were fractionated via strong cation exchange (SCX) chromatography on a 20AD high-performance liquid chromatography (HPLC) system (Shimadzu; Kyoto, Japan) using a polysulfoethyl column (2.1 × 100 mm, 5 μm, 200 Å, Poly LC, Columbia, MD). Peptides were eluted with a linear gradient of 0–500 mM KCl (10 mM KH_2PO_4 in 25 % v/v acetonitrile, pH 2.6) for 60 min at a flow rate of 200 μL/min. In total, twenty fractions were collected.

Each fraction was dried, dissolved in 0.1 % FA (formic acid) aqueous solution, and analyzed on a QSTAR XL system (Applied Biosystems, China) interfaced with a 20AD HPLC system (Shimadzu, Kyoto, Japan). Peptides were separated on a reverse-phase Zorbax 300SB-C18 column (75 × 150 mm, 3 μm, 100 Å, Microm, Auburn, CA). The mobile phase was composed of 0.5 % formic acid in water (A) and acetonitrile (B). The flow rate was 400 nL/min with a gradient from 5 % to 45 % B over 70 min and 90 % B over 10 min. MS data were acquired automatically using Analyst QS 1.0 software Service Pack 8 (ABI/MDS SCIEX, Concord, Canada). Survey scans were acquired from 400 to 1800, with up to 4 precursors selected for MS/MS from m/z 100 to 2000. Curtain gas was set at 10, nitrogen was used as the collision gas, and the ionization tip voltage was 4000 V.

Data analysis

Relative quantification and protein identification were performed with ProteinPilot[TM] software (version 3.0, revision 114732, Applied Biosystems) using the Paragon[TM] algorithm as the search engine. Each MS/MS spectrum was searched against a database of Sus scrofa protein sequences (NCBI nr, released March 2008, downloaded from ftp.ncbi.nih.gov/genomes/Sus_scrofa/protein/). The search parameters allowed for cysteine modification by methyl methanethiosulfonate, and biological modifications were programmed in the algorithm (i.e., amidation, phosphorylation, and semitryptic fragments). All identified proteins required ≥95 % confidence, and the protein confidence threshold cutoff was set to 1.3 (unused) with at least more than one peptide above the 95 % confidence level. The true value for the average ratio was expressed as an error factor (EF = 10 (95 % confidence interval)) and calculated according to the reports. EF <2 was set for satisfactory quantification quality. To designate significant changes in protein expression, fold-changes >1.25 or <0.75 were set as cutoff values. To decrease artificial error, the bias correction option was executed. In addition, one-way analysis of variance (ANOVA) and LSD analysis (SPSS 18.0) were used to determine whether the protein was significantly regulated over time. Differences were considered statistically significant for P values <0.05.

Bioinformatics

Proteins that met the criteria for differential expression were compared with hierarchical cluster analysis using Cluster 3.0 program [19]. Data were displayed using Java Tree View [20]. The molecular functions and subcellular localizations of the unique proteins identified were classified using Protein Center software (DAVID Functional Annotation Tools) [21, 22]. The main annotation types were obtained from the gene ontology consortium Web site (http://david.abcc.ncifcrf.gov/). The protein–protein interaction network was analyzed via STRING software (http://string.embl.de/) [23].

Immunofluorescence assay (IFA)

PCV2 infected cells were washed with PBS, fixed with cold acetone/methanol (1/1 v/v) for 20 min at −20 °C, and allowed to air-dry. Fixed cells were incubated with pig anti-PCV2 polyclonal antiserum (VMRD, USA) at 37 °C for 1 h, washed three times with PBST (0.05 % Tween-20 in PBS, pH 7.4), and further incubated with staphylococcal protein A (SPA) conjugated to FITC (Boshide, Wuhan, China) at 37 °C for 1 h in the dark. After three washes with PBST, infected cells were quantified using Zeiss LSM510 laser confocal microscopy.

Western blot

Samples of PCV2-infected and uninfected PK-15 cells were lysed at 12, 24, 48, and 96 hpi (hours post-infection), and the protein concentrations determined with the Pierce BCA Protein Assay Kit (Thermo Scientific, Product No. 23227, USA). Equivalent amounts of cell lysate proteins were subjected to 12 % SDS-PAGE and transferred to 0.22 μm nitrocellulose membranes (Hybond-C extra, Amersham Biosciences). After blotting, membranes were incubated at 37 °C for 60 min, respectively, with mouse monoclonal antibodies (mAbs) to actin (Abcam, Cambridge, UK), vimentin (Santa Cruz Biotechnology, CA), Ras-related protein Rab-11A (Santa Cruz Biotechnology, CA), Hsp90 (Abcam, Cambridge, UK), PCV2 Cap protein (made in our laboratory), or rabbit polyclonal antibody to AnnexinI (Santa Cruz Biotechnology, CA). After washing three times with 0.05 % PBST, membranes were incubated
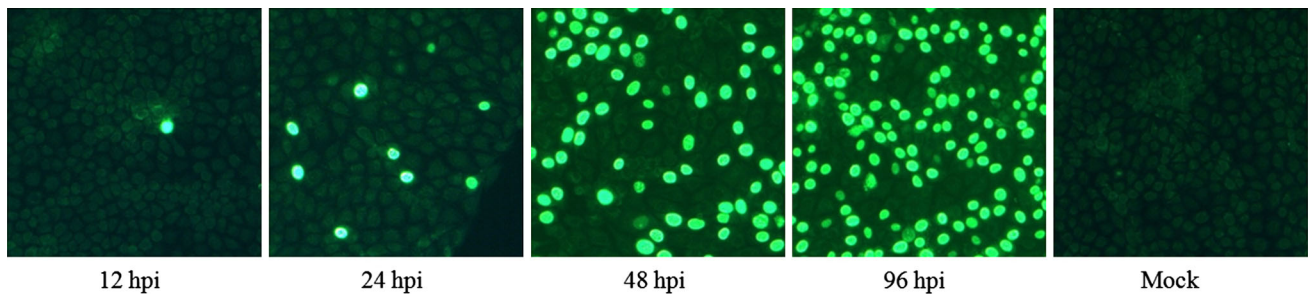
| 12 hpi | 24 hpi | 48 hpi | 96 hpi | Mock |

Fig. 2 Detection of PCV2 in PK-15 cells with IFA. Cells inoculated with the PCV2 WG09 strain at 1 MOI and mock-infected cells were collected at 12, 24, 48, and 96 hpi, respectively. After fixing with cold acetone/methanol, cells were incubated with swine serum antibody to PCV2 and subsequently with FITC-labeled SPA (1:50). After washing, cells were examined using fluorescence microscopy (Zeiss LSM510)

at 37 °C for 60 min with horseradish peroxidase-conjugated goat anti-mouse IgG (Boshide, Wuhan, China) or goat anti-rabbit IgG (Boshide, Wuhan, China). Detection was performed using chemiluminescence luminol reagents (SuperSignalWest PicoTrial Kit, Pierce). Protein spot levels were determined using ImageJ quantification software.

Results

Confirmation of PCV2 propagation in PK-15 via IFA

Since PCV2 does not induce a typical cytopathic effect (CPE) in PK-15 cells, viral infection was confirmed by detection of PCV2 antigen using IFA at 12, 24, 48, and 96 hpi. The results clearly revealed green fluorescence in PCV2-infected PK-15 cells, which was absent in mock-infected cells. Fluorescence microscopy observations indicated that PCV2 titers increase during the first 24 h of infection, and 70–80 % of cells treated with PCV2 are infected at 96 hpi (Fig. 2).

Protein profile with iTRAQ-coupled 2D LC–MS/MS analysis

Protein extracts were prepared separately from PCV2-infected PK-15 cells at 12, 24, 48, and 96 hpi and virus-free PK-15 cells at the same time points as the mock control group. Overall, 711 proteins were detected using iTRAQ-coupled 2D LC–MS/MS analysis. Among these, 196 proteins displayed significantly altered expression post-infection. As shown in Fig. 3 and Table 1, significantly altered proteins were divided into eight clusters: (1) up-regulated only, (2) down-regulated only, (3) up-down regulated, (4) down-up regulated, (5) up-down-up regulated, (6) down-up-down regulated, (7) up-down-up-down regulated, and (8) down-up-down-up regulated.

Functional classification of identified proteins

Functional annotation of the 196 proteins that were significantly altered after infection of PK-15 cells with PCV2 was initially performed using Protein Center software. Three main annotation types were obtained from the gene ontology consortium Web site: Biological Processes, Subcellular Location, and Molecular Function. Enrichment analysis of biological processes showed that PCV2 infection primarily affects the generation of precursor metabolites and energy (Fig. 4a) and revealed nucleotide-binding, cytoskeletal protein binding, and hydrolyase activity as the commonly affected metabolic functions in PCV2-infected PK-15 cells (Fig. 4c). Furthermore, cellular component-based enrichment analysis showed that proteins with significant alterations are differentially distributed in cells (Fig. 4b).

Protein–protein interactions

Interactions between the virus and host cell are complex and mutual when a virus invades the host. Next, we aimed to determine how PCV2 interacts with PK-15 cell proteins and the effects of these interactions on cell function. The STRING database was searched for interactions with significantly altered proteins in response to PCV2 infection (Fig. 5). The analysis revealed several proteins with interesting interactions, including Hspa12a-Hyou1-Hspa5-Hspd1-Rsp16-Rsp18-Rpl5 and Canx-Calx-Ppib-Ppl10-Prdx2-Anxa2-Anxa1-Vim. These seed proteins play important functions in signal transduction and cell adhesion. For example, Anxa2 is a RNA-binding protein implicated in several cellular transport processes, including internalization and transport of cholesteryl esters, biogenesis of multivesicular bodies, recycling of plasma membrane receptors, and Ca^{2+}-induced exocytosis of specific secretory granules [24].

Fig. 3 Hierarchical cluster analysis for proteins revealed significant alterations in expression levels at different time-courses post-infection. Protein expression is shown using a pseudocolor scale (from −3 to 3), with *red* indicating high expression and *green* signifying low expression (Color figure online)

-3.0   0.0   3.0

12h   24h   48h   96h

gi|350583632 // PREDICTED: calponin-3
gi|56748897 // Heat shock 70 kDa protein 1B
gi|350594189 // cadherin-6;cadherin-10
gi|311264042 // PREDICTED: hypoxia up-regulated protein 1
gi|162951821 // heterogeneous nuclear ribonucleoprotein A/B
gi|350588024 // heterogeneous nuclear ribonucleoprotein D0
gi|31124796 // PREDICTED: apoptosis inhibitor 5 isoform 1
gi|194034833 // PREDICTED: microfibrillar-associated protein 1
gi|335295652 // laminin subunit beta-1
gi|335284315 // PREDICTED: RNA-binding protein FUS-like isoform 2
gi|350584416 // PREDICTED: parathymosin-like
gi|194044922 // ADP/ATP translocase 2
gi|350594172 // brain acid soluble protein 1-like isoform 2
gi|335299026 // microtubule-associated protein 4-like
gi|83921635 // FKBP1A-like
gi|7503972 // Unconventional myosin-VI
gi|408360214 // Vimentin
gi|350586335 // nuclease-sensitive element-binding protein 1
gi|335280113 // LOW QUALITY PROTEIN: 60S ribosomal protein L4
gi|350582932 // annexin A13 isoform 2
gi|346421378 // serpin H1 precursor
gi|350529387 // basic transcription factor 3
gi|358009193 // prolyl 4-hydroxylase beta polypeptide
gi|178056236 // RNA-binding protein 4B
gi|60394813 // 40S ribosomal protein S16
gi|213983067 // 60S ribosomal protein L26-like 1
gi|311252000 // fumarylacetoacetate hydrolase domain-containing protein 2
gi|335284299 // T-complex protein 1 subunit zeta-like isoform 1
gi|350578257 // heterogeneous nuclear ribonucleoprotein Q isoform 1
gi|346986388 // profilin-1
gi|85681889 // 60S ribosomal protein L10
gi|389818965 // U2 small nuclear RNA auxiliary factor 2
gi|350594669 // PREDICTED: ribosome-binding protein 1
gi|7939586 // dihydrolipoamide succinyltransferase
gi|311254317 // cingulin-like alpha
gi|343478174 // T-complex protein 1 subunit alpha
gi|194041525 // dihydropyrimidinase-related protein 2
gi|178056550 // D-3-phosphoglycerate dehydrogenase
gi|61216107 // Adenosylhomocysteinase;
gi|335286747 // hepatoma-derived growth factor-like
gi|51317314 // Histone H4
gi|213958609 // glutamine:fructose-6-phosphate amidotransferase 1 variant 2
gi|281427370 // T-complex protein 1 subunit eta
gi|47522630 // aspartate aminotransferase, mitochondrial precursor
gi|350594033 // UDP-glucuronosyltransferase 1-10 isoform 2
gi|194403605 // PREDICTED: GTP-binding nuclear protein Ran
gi|335309827 // nuclear autoantigenic sperm protein, partial
gi|172072661 // tRNA-splicing ligase RtcB homolog
gi|349501107 // ribosomal protein, large, P2
gi|350535040 // eukaryotic translation initiation factor 4 gamma 1
gi|311249564 // heterogeneous nuclear ribonucleoprotein H
gi|273463176 // cell division cycle 2 variant 1
gi|158517860 // Thymosin beta-10; AltName: Thymosin beta-9
gi|350576057 // 78 kDa glucose-regulated protein
gi|55983054 // proteasome 26S subunit non-ATPase 4
gi|347582591 // cytoskeleton-associated protein 4
gi|54039746 // Tropomyosin alpha-4 chain
gi|350591535 // PREDICTED: hypothetical protein LOC100522278
gi|350591320 // 26S proteasome non-ATPase regulatory subunit 6
gi|350579350 // stomatin-like protein 2-like
gi|54039123 // 60S ribosomal protein L22
gi|335305558 // heterogeneous nuclear ribonucleoproteins A2/B1
gi|340007404 // alpha-actinin-1
gi|329663948 // ras GTPase-activating protein-binding protein 1
gi|311250943 // PREDICTED: 28 kDa heat- and acid-stable phosphoprotein
gi|350595802 // SH3 domain-binding glutamic acid-rich-like protein-like
gi|335309813 // PREDICTED: coactosin-like protein-like, partial
gi|346644699 // protein SET
gi|350578528 // peptidyl-prolyl cis-trans isomerase B
gi|311261216 // c-1-tetrahydrofolate synthase, cytoplasmic
gi|374637318 // heart fatty acid-binding protein
gi|194037005 // m7GpppX diphosphatase; AltName: DCS-1
gi|85792232 // eukaryotic translation initiation factor 4A
gi|212549625 // 40S ribosomal protein S3a
gi|75069665 // ADP-ribosylation factor-like protein 1
gi|350529411 // proteasome (prosome, macropain) 26S subunit
gi|393714792 // sodium/potassium-transporting ATPase subunit alpha-1
gi|350583346 // ubiquitin associated protein 2-like isoform 3
gi|311250313 // histidyl-tRNA synthetase, cytoplasmic
gi|350592730 // heterogeneous nuclear ribonucleoprotein F
gi|347658971 // ATP synthase, H+ transporting,
gi|335282599 // PREDICTED: interleukin enhancer-binding factor 3
gi|335293906 // annexin A5-like
gi|178056781 // histone H2A.Z
gi|94421332 // putative aldo-keto reductase family 1 member C4
gi|350583022 // 14-3-3 protein zeta/delta
gi|311252547 // T-complex protein 1 subunit delta-like
gi|28948618 // Annexin A1
gi|350594505 // PREDICTED: annexin A6-like
gi|281500757 // Porcine Aldehyde Reductase In Ternary Complex With Inhibitor
gi|359811347 // 60 kDa heat shock protein, mitochondrial
gi|350580027 // elongation factor 1-gamma
gi|350580371 // 40S ribosomal protein S18
gi|115502828 // 40S ribosomal protein S3
gi|350592730 // CDC37 cell division cycle 37 protein
gi|311245228 // PREDICTED: serpin B5
gi|345441771 // aldolase C, fructose-bisphosphate
gi|473575 // lactate dehydrogenase-B
gi|75074817 // Peroxiredoxin-6
gi|34234919 // calnexin
gi|9857227 // ribophorin I
gi|335284210 // Heat shock protein beta-1;Short=HSP 27
gi|4033507 // Annexin A4
gi|335291884 // histone H2B type 1-like
gi|335306989 // ATP-dependent RNA helicase A-like
gi|25568304 // isocitrate dehydrogenase [NADP], mitochondrial
gi|346644805 // pinin
gi|194034450 // nidogen-2
gi|347300243 // glutamate dehydrogenase 1, mitochondrial
gi|387912908 // Calreticulin
gi|335284690 // PREDICTED: periplakin
gi|350594261 // NAD(P) transhydrogenase, mitochondrial-like
gi|343432604 // ubiquitin-conjugating enzyme E2 variant 2
gi|8745552 // voltage-dependent anion channel 1
gi|87047845 // nm23-H2,nucleoside diphosphate kinase B
gi|54037185 // Guanine nucleotide-binding protein subunit beta-2-like
gi|97190495 // Protein S100-A6; AltName: Calcyclin
gi|194036918 // thiosulfate sulfurtransferase
gi|350586583 // serine/arginine-rich splicing factor 3-like
gi|346716324 // myosin regulatory light chain 2 protein isoform 2
gi|48675927 // tropomyosin alpha-3 chain
gi|90200404 // triosephosphate isomerase 1
gi|194595733 // clathrin light chain (CLTA) protein
gi|51592135 // cofilin-1
gi|1709973 // 60S ribosomal protein L10a
gi|57527987 // moesin
gi|194037005 // PREDICTED: ribonuclease UK114-like isoform 1
gi|9739517 // macrophage migration inhibitory factor, partial
gi|335285943 // eukaryotic translation initiation factor 5A-1-like
gi|194037373 // coatomer subunit zeta-1 isoform 1
gi|311272155 // activated RNA polymerase II transcriptional coactivator p15
gi|343887420 // transcription elongation factor A protein 1
gi|335290365 // 45 kDa calcium-binding protein-like
gi|350595172 // PREDICTED: UPF0562 protein C7orf55 homolog
gi|347300276 // poly(rC) binding protein 2
gi|219522018 // Na(+)/H(+) exchange regulatory cofactor NHE-RF1
gi|47523692 // thioredoxin
gi|45268967 // 40S ribosomal protein S28, partial
gi|194044626 // 14-3-3 protein beta/alpha isoform 1
gi|345199274 // glutaredoxin 3
gi|342672022 // exportin-2
gi|335306870 // PREDICTED: protein S100-A2-like
gi|311273021 // fibronectin isoform 2
gi|346888432 // ras homolog gene family, member A
gi|194044484 // eukaryotic translation initiation factor 2 subunit 2
gi|54036319 // 40S ribosomal protein S17
gi|346644746 // calmodulin 1
gi|350585373 // myosin-14-like
gi|350590594 // malate dehydrogenase, cytoplasmic-like
gi|350580630 // far upstream element-binding protein 2-like
gi|335281298 // PREDICTED: tubulin beta-2C chain-like
gi|346227222 // ribosomal protein L13a isoform 1
gi|47523618 // citrate synthase, mitochondrial precursor
gi|51702768 // Peptidyl-prolyl cis-trans isomerase A
gi|83854099 // ribosomal phosphoprotein large P0 subunit
gi|350578507 // asparaginyl-tRNA synthetase, cytoplasmic-like
gi|350585579 // alpha-enolase-like, partial
gi|350596533 // PREDICTED: copper transport protein ATOX1-like, partial
gi|311245734 // PREDICTED: hypothetical protein LOC100038023
gi|311248936 // phenylalanyl-tRNA synthetase alpha chain-like
gi|346227216 // ribosomal protein L15
gi|350578005 // ezrin
gi|346227212 // ribosomal protein L3
gi|54020906 // annexin A2
gi|346986428 // heat shock 90kD protein 1, beta
gi|347300176 // peroxiredoxin-2
gi|345441750 // heat shock 70kDa protein 8
gi|335282386 // elongation factor 2
gi|350585766 // chloride intracellular channel protein 4-like
gi|311267276 // keratin, type I cytoskeletal 19-like
gi|223019599 // eukaryotic translation elongation factor 1 alpha 1
gi|75056558 // Ras-related protein Rab-11A;
gi|81174748 // beta 5-tubulin
gi|194038728 // pyruvate kinase isozymes M1/M2 isoform 1
gi|319401915 // rho GDP-dissociation inhibitor 1
gi|346986294 // uncharacterized protein LOC100155717 isoform 2
gi|350584132 // PREDICTED: proliferation-associated protein 2G4
gi|335300686 // PREDICTED: carbonyl reductase [NADPH] 1-like
gi|311273095 // ATP-binding cassette sub-family B member 6, mitochondrial
gi|350579323 // retinal dehydrogenase 1-like, partial
gi|343887407 // thiopurine S-methyltransferase
gi|8745554 // voltage-dependent anion channel 2
gi|166796061 // 60S ribosomal protein L5
gi|350595677 // PREDICTED: spermine synthase
gi|343403779 // ribosomal protein L13
gi|85542092 // 60S ribosomal protein L6
gi|75073672 // Calcium/calmodulin-dependent protein kinase type II
gi|335284397 // major vault protein isoform 1
gi|227430407 // keratin, type II cytoskeletal 8
gi|157279735 // succinate dehydrogenase [ubiquinone] iron-sulfur subunit
gi|349585075 // small acidic protein
gi|50403675 // Vinculin; AltName: Metavinculin
gi|311247012 // epidermal growth factor receptor kinase substrate 8
gi|347300323 // thioredoxin-dependent peroxide reductase, mitochondrial
gi|350591497 // PREDICTED: ras-related protein Rab-7a-like
gi|304365428 // protein disulfide-isomerase A3 precursor

Table 1 Statistically significant differentially expressed proteins identified by iTRAQ analysis of PK-15 cells infected with PCV2

Accession	Protein name	Ratio				P value	% Cov (95%)	Peptides (95 %)	Function
		12 hpi	24 hpi	36 hpi	48 hpi				
Cluster 1: up-regulation (63)									
gi|345441750	Heat shock 70 kDa protein 8	0.98	1.03	**1.56**	**2.96**	4.58E−8	45.05	43	Repressor of transcriptional activation
gi|346986428	Heat shock 90kD protein 1	0.88	1.11	1.18	**2.13**	3.59E−7	32.73	31	Stress response
gi|350579657	78–kDa glucose-regulated protein	**1.56**	**1.46**	**1.34**	1.08	1.79E−5	37.03	31	Facilitate the assembly of multimeric protein
gi|358009193	Prolyl 4-hydroxylase beta polypeptide	1.17	1.11	1.07	**1.64**	6.74E−6	37.40	28	Cell redox homeostasis
gi|335282386	Elongation factor 2	1.01	0.98	1.22	**2.51**	4.58E−8	20.51	16	Translational elongation
gi|335293906	Annexin A5	0.99	1.18	**1.56**	1.14	6.01E−7	42.37	20	Calcium ion binding
gi|359811347	60-kDa heat shock protein	1.08	**1.36**	**1.53**	**1.66**	5.28E−7	23.73	19	Chaperone-mediated protein complex assembly
gi|350578005	Ezrin	0.86	0.81	**1.32**	**1.87**	3.51E−8	21.21	14	Cytoskeletal anchoring at plasma membrane
gi|473575	Lactate dehydrogenase-B	0.83	**1.33**	**1.66**	**1.36**	1.48E−7	26.05	10	Cellular carbohydrate metabolic process
gi|223019599	Eukaryotic translation elongation factor 1	1.00	1.16	**1.42**	**1.72**	2.11E−7	21.00	17	Translation elongation factor activity
gi|81174748	Beta 5-tubulin	0.79	1.08	**1.72**	**1.58**	5.91E−8	24.32	16	Structural constituent of cytoskeleton
gi|54036319	40S Ribosomal protein S17	1.00	0.87	**3.25**	0.99	1.19E−9	17.04	6	rRNA processing
gi|350586583	Serine/arginine-rich splicing factor 3	**2.29**	0.78	**1.31**	1.07	1.13E−8	17.68	3	mRNA splicing, via spliceosome
gi|75074817	Peroxiredoxin-6	0.77	1.11	**1.39**	1.21	4.51E−7	41.07	18	Redox regulation of the cell
gi|56748897	Heat shock 70 kDa protein 1B	**1.37**	1.17	0.79	**1.34**	4.11E−7	32.76	23	Stress response
gi|387912908	Calreticulin	0.81	**1.32**	**1.38**	1.24	4.68E−7	17.51	8	Calcium ion binding
gi|311252547	T-complex protein 1 subunit delta	0.94	**1.26**	**1.33**	**1.58**	4.30E−7	12.80	7	ATP binding
gi|51702768	Peptidyl-prolyl cis–trans isomerase A	1.25	1.00	**1.63**	**1.26**	4.58E−7	38.41	10	PPIases accelerate the folding of proteins
gi|350583022	14-3-3 protein zeta/delta	0.79	**1.32**	**1.53**	**2.21**	1.70E−8	38.37	13	Cellular membrane organization
gi|194038728	Pyruvate kinase isozymes M1/M2	0.78	1.07	**1.71**	**1.71**	4.32E−8	48.21	39	Pyruvate kinase activity
gi|350579323	Retinal dehydrogenase 1	0.85	0.90	**1.60**	**1.63**	6.21E−8	15.56	5	Convert/oxidize retinaldehyde to retinoic acid
gi|83854099	Ribosomal phosphoprotein large PO subunit	**1.36**	1.10	**1.74**	**1.42**	4.34E−7	21.70	7	Structural constituent of ribosome
gi|194044922	ADP/ATP translocase 2	**1.72**	1.20	0.78	1.20	9.49E−8	20.47	7	Adenine transmembrane transporter activity
gi|343478174	T-complex protein 1 subunit alpha	0.79	**1.46**	1.20	**1.39**	2.54E−7	13.49	8	ATP binding
gi|281427370	T-complex protein 1 subunit eta	0.88	1.18	1.08	**1.33**	1.63E−6	9.39	5	Binding of sperm to zona pellucida
gi|194044484	Eukaryotic translation initiation factor 2 subunit 2	1.05	0.89	**3.40**	**1.27**	1.09E−9	23.72	5	Eukaryotic translation initiation factor 2 complex
gi|349501107	Ribosomal protein, large, P2	**1.49**	1.14	**1.39**	0.77	1.96E−7	60.00	6	Protein kinase activity
gi|335285943	Eukaryotic translation initiation factor 5A-1	**1.49**	0.92	**1.46**	1.07	3.33E−7	40.91	8	Positive regulation of translational elongation
gi|374637318	Heart fatty acid-binding protein	1.17	**2.40**	**1.43**	**1.31**	2.14E−8	31.58	5	Fatty acid metabolic process
gi|347582591	Cytoskeleton-associated protein 4	**1.96**	**1.32**	**1.38**	0.86	5.03E−8	13.85	5	High-affinity epithelial cell surface receptor for APF
gi|350592730	Heterogeneous nuclear ribonucleoprotein F	0.91	1.19	**1.60**	1.01	2.41E−7	18.36	8	mRNA processing

Table 1 continued

Accession	Protein name	Ratio				P value	% Cov (95%)	Peptides (95 %)	Function
		12 hpi	24 hpi	36 hpi	48 hpi				
gi|335280113	60S ribosomal protein L4	**1.38**	0.79	1.12	**4.29**	3.10E−10	5.39	3	Translational elongation
gi|389618965	U2 small nuclear RNA auxiliary factor 2	0.97	**1.26**	0.88	**1.53**	2.74E−7	3.40	2	Nucleotide binding
gi|346644746	Calmodulin 1	**1.29**	1.24	**4.33**	**1.42**	4.02E−10	34.90	11	Calcium ion binding
gi|311273095	ATP binding cassette sub-family B member 6	0.86	0.95	**1.49**	**1.37**	2.27E−7	2.09	2	Cadmium ion transmembrane transport
gi|54039746	Tropomyosin alpha-4 chain	**1.50**	1.15	1.10	0.94	6.70E−7	18.55	6	Muscle filament sliding
gi|350583632	Calponin-3	**1.37**	1.22	0.90	**1.56**	3.44E−7	16.72	4	Actomyosin structure organization
gi|319401915	Rho GDP-dissociation inhibitor 1	0.78	1.06	**1.61**	**1.71**	5.35E−8	29.90	7	Rho protein signal transduction
gi|115502828	40S ribosomal protein S3	0.83	1.10	**1.46**	**1.61**	1.34E−7	20.16	5	DNA-(apurinic or apyrimidinic site) lyase activity
gi|350584132	Proliferation-associated protein 2G4	0.87	0.85	**2.19**	**1.79**	1.01E−8	19.57	4	ERBB3-regulated signal transduction pathway
gi|346986388	Profilin-1	0.88	1.03	0.90	**1.82**	5.23E−8	52.14	9	Actin cytoskeleton organization
gi|47523692	Thioredoxin	**1.45**	0.97	**1.57**	0.95	1.95E−7	29.52	8	Possesses a dithiol-reducing activity
gi|194036918	Thiosulfate sulfurtransferase	**2.25**	0.92	1.29	1.15	1.77E−8	24.09	3	Sulfur amino acid catabolic process
gi|350529387	Basic transcription factor 3	**1.46**	1.17	1.28	**4.09**	5.44E−10	24.07	5	Transcription regulatory region DNA binding
gi|347658971	ATP synthase, H + transporting, mitochondrial Fo complex	0.79	1.15	**1.54**	0.83	1.42E−7	33.54	4	Mitochondrial ATP synthesis coupled proton transport
gi|346227212	Ribosomal protein L3	0.89	1.14	1.13	**1.87**	6.42E−8	8.69	4	Structural constituent of ribosome
gi|178056236	RNA-binding protein 4B	0.88	0.88	0.82	**1.47**	2.36E−7	7.52	3	Nucleotide binding
gi|54039371	40S ribosomal protein S18	0.89	**1.26**	**1.69**	**1.87**	5.53E−8	21.05	3	rRNA binding
gi|87047646	nm23-H2, nucleoside diphosphate kinase B	0.99	**1.98**	**1.49**	**1.32**	7.18E−8	24.34	3	GTP biosynthetic process
gi|212549625	40S ribosomal protein S3a	0.88	**1.75**	1.25	0.86	6.87E−8	7.95	2	Ribonucleoprotein complex
gi|213983067	60S ribosomal protein L26	1.24	1.03	0.86	**1.96**	3.79E−8	17.24	3	Ribosomal large subunit biogenesis
gi|197190495	Protein S100-A6	**2.15**	0.94	1.20	1.03	2.16E−8	16.67	2	Signal transduction
gi|54037165	Guanine nucleotide-binding protein subunit beta-2	0.88	**1.45**	1.15	1.10	6.42E−7	7.89	2	G-protein coupled receptor signaling pathway
gi|335306870	Protein S100-A2	**1.27**	1.17	**1.91**	1.10	1.09E−7	16.49	2	Endothelial cell migration
gi|349585075	Small acidic protein	1.13	0.79	**1.72**	**1.56**	6.59E−8	21.55	7	Regulation of gene expression, epigenetic
gi|350595172	UPF0562 protein C7orf55 homolog	**1.94**	1.03	**1.91**	0.83	1.83E−8	8.08	4	Belongs to the UPF0562 family
gi|166796061	60S ribosomal protein L5	1.06	1.00	**1.54**	**1.74**	1.20E−7	6.40	2	Ribosomal large subunit biogenesis
gi|350580630	Far upstream element-binding protein 2	1.07	0.85	**1.61**	0.91	1.45E−7	5.76	4	mRNA processing
gi|1709973	60S ribosomal protein L10a	**1.63**	1.03	**1.43**	**1.43**	5.18E−7	13.33	3	RNA binding
gi|75073672	Calcium/calmodulin-dependent protein kinase type II	1.06	1.10	**1.77**	**2.65**	1.52E−9	5.81	2	Calcium ion transport
gi|350596533	Copper transport protein ATOX1	**1.33**	0.78	**1.96**	**1.31**	3.83E−8	31.82	2	Response to oxidative stress

Table 1 continued

Accession	Protein name	Ratio 12 hpi	24 hpi	36 hpi	48 hpi	P value	% Cov (95%)	Peptides (95 %)	Function
gi|178056781	Histone H2A.Z	0.85	1.41	1.54	1.64	1.34E-7	31.25	6	Nucleosome assembly
gi|158517860	Thymosin beta-10	1.43	1.27	1.29	0.99	1.80E-6	50.00	5	Actin cytoskeleton organization
Cluster 2: down-regulation (49)									
gi|311273021	Fibronectin isoform 2	0.70	0.65	1.10	0.85	1.24E-6	13.20	30	Matrix organization of cartilage
gi|47523618	Citrate synthase	0.89	0.66	1.22	0.86	7.18E-7	7.76	3	ATP catabolic process
gi|311267276	Keratin type I cytoskeletal 19	0.58	0.68	0.79	1.00	1.16E-6	56.19	27	Organization of myofibers
gi|227430407	keratin, type II cytoskeletal 8	0.60	0.30	0.85	1.11	1.44E-7	33.54	21	Cell morphogenesis involved in differentiation
gi|347300243	Glutamate dehydrogenase 1	0.43	0.94	1.03	0.98	3.42E-7	24.01	14	Cellular amino acid metabolic process
gi|157279735	Succinate dehydrogenase [ubiquinone] iron–sulfur subunit	0.59	0.34	1.04	1.00	1.62E-7	6.07	2	Electron transport
gi|55983054	Proteasome 26S subunit non-ATPase 4	1.21	0.74	0.58	0.31	1.02E-7	11.14	2	mRNA metabolic process
gi|350594261	NAD(P) transhydrogenase	0.27	0.95	0.83	0.88	2.19E-7	2.19	2	Reactive oxygen species metabolic process
gi|343887420	Transcription elongation factor A protein 1	1.14	0.65	1.08	0.65	4.11E-7	4.00	3	C2H2 zinc finger domain binding
gi|5739517	Macrophage migration inhibitory factor	1.13	0.55	0.90	0.65	4.51E-7	16.22	4	Pro-inflammatory cytokine
gi|219522018	Na(+)/H(+) exchange regulatory cofactor NHE-RF1	0.99	0.65	0.84	0.63	2.46E-6	6.85	2	Wnt receptor signaling pathway
gi|346986432	ras homolog gene family, member A	0.69	0.65	1.05	0.79	1.98E-6	12.95	3	Rho protein signal transduction
gi|350594505	Annexin A6	0.44	0.75	0.87	1.07	4.30E-7	3.79	3	Regulate the release of Ca^{2+} from intracellular stores
gi|57527987	Moesin	0.93	0.58	0.66	0.80	3.63E-6	20.80	13	Structural constituent of cytoskeleton
gi|335284397	Major vault protein isoform 1	0.64	0.38	0.76	0.86	1.12E-6	18.56	15	Protein transport
gi|335305558	Heterogeneous nuclear ribonucleoproteins A2/B1 isoform 1	1.09	1.16	0.98	0.59	4.97E-7	43.91	16	pre-mRNA intronic binding
gi|393714792	Sodium/potassium-transporting ATPase subunit alpha-1	0.65	1.00	1.18	0.54	2.62E-7	17.45	16	Sodium/potassium transport
gi|311261216	c-1-tetrahydrofolate synthase	0.54	0.68	0.53	0.51	5.65E-5	10.37	8	Formate-tetrahydrofolate ligase activity
gi|335306989	ATP-dependent RNA helicase A	0.45	0.89	0.86	0.70	1.26E--6	5.99	6	Putative ATP-dependent RNA helicase
gi|335299026	Microtubule-associated protein 4	1.11	0.64	0.42	0.92	2.43E-7	6.57	5	Promotes microtubule assembly
gi|350582932	Annexin A13	0.60	0.49	0.60	1.00	4.82E-7	19.63	6	Calcium ion binding
gi|50403675	Vinculin	0.65	0.47	1.10	0.97	2.99E-7	6.43	6	Cell–matrix adhesion and cell–cell adhesion
gi|350535040	Eukaryotic translation initiation factor 4 gamma 1	0.82	0.65	0.79	0.35	9.76E-7	4.13	6	Regulation of translational initiation
gi|329663948	ras GTPase-activating protein-binding protein 1	0.96	0.96	0.86	0.42	4.37E-7	15.27	7	ATP-dependent DNA helicase activity
gi|178056550	D-3-phosphoglycerate dehydrogenase	0.65	1.06	0.89	0.96	2.23E-6	9.76	4	Amino acid biosynthesis

Table 1 continued

Accession	Protein name	Ratio				P value	% Cov (95%)	Peptides (95 %)	Function
		12 hpi	24 hpi	36 hpi	48 hpi				
gi|311254317	Cingulin	0.39	0.68	0.57	0.68	5.91E−6	3.18	4	Cell junction
gi|61216107	Adenosylhomocysteinase	0.57	1.20	0.77	0.94	4.35E−7	11.34	5	S-adenosylhomocysteine catabolic process
gi|347300176	Peroxiredoxin-2	0.59	0.65	0.71	0.95	3.34E−6	18.69	5	Involved in redox regulation of the cell
gi|311264042	Hypoxia up-regulated protein 1	1.08	1.14	0.53	1.07	3.15E−7	4.81	5	A molecular chaperone and participate in protein folding
gi|194041525	Dihydropyrimidinase-related protein 2	0.26	0.94	0.56	0.79	2.76E−7	7.24	3	Axon guidance
gi|72072661	tRNA-splicing ligase RtcB homolog	1.09	1.10	0.66	0.50	1.00E−6	7.33	3	tRNA splicing, via endonucleolytic cleavage and ligation
gi|347300323	Thioredoxin-dependent peroxide reductase	1.06	0.47	1.25	1.14	1.40E−7	17.62	4	Involved in redox regulation of the cell
gi|194037005	Ribonuclease UK114	1.09	0.26	0.33	0.73	9.86E−8	38.69	4	Nucleic acid phosphodiester bond hydrolysis
gi|350594033	UDP-glucuronosyltransferase 1-10 isoform 2	0.54	0.83	0.75	1.13	5.82E−7	6.60	3	Glucuronosyltransferase activity
gi|75039721	Unconventional myosin-VI	0.64	0.58	0.57	0.74	5.54E−5	4.23	4	Actin-based motor molecules with ATPase activity
gi|350595577	Spermine synthase	0.89	0.64	0.93	1.16	1.01E−6	9.90	3	Spermine biosynthetic process
gi|7939586	Dihydrolipoamide succinyltransferase	0.72	1.05	0.65	0.91	1.89E−6	4.61	2	Cellular nitrogen compound metabolic process
gi|335284690	Periplakin	0.25	1.24	1.16	0.95	5.06E−8	1.71	3	Structural constituent of cytoskeleton
gi|350585766	Chloride intracellular channel protein 4	0.63	0.70	0.86	1.11	1.01E−6	25.19	5	Branching morphogenesis of an epithelial tube
gi|335286747	Hepatoma-derived growth factor	0.53	1.10	0.75	0.92	5.95E−7	20.58	3	Acts as a transcriptional repressor
gi|273463176	Cell division cycle 2 variant 1	0.79	0.66	0.62	0.27	8.53E−7	11.45	3	Regulation of transcription, DNA–dependent
gi|311272155	Activated RNA polymerase II transcriptional coactivator p15	0.98	0.54	1.10	0.65	4.19E−7	25.98	4	Transcription, DNA-dependent
gi|94421332	Putative aldo–keto reductase family 1 member C4	0.45	0.90	0.97	1.18	2.19E−7	8.70	2	Oxido reductase activity
gi|311250313	Histidyl-tRNA synthetase	0.59	0.75	1.07	0.60	8.26E−7	3.93	2	tRNA aminoacylation for protein translation
gi|54039123	60S ribosomal protein L22	0.88	1.15	0.94	0.43	2.47E−7	18.75	2	Translation
gi|347300276	poly(rC)-binding protein 2	1.03	0.77	0.94	0.67	2.97E−6	8.78	4	Immunity
gi|335300686	Carbonyl reductase [NADPH] 1	0.64	0.64	1.09	0.99	6.87E−7	11.03	3	Carbonyl reductase (NADPH) activity
gi|194595733	Clathrin light chain (CLTA) protein	1.25	0.55	0.87	0.91	3.09E−7	33.54	7	Cellular membrane organization
gi|340007404	Alpha-actinin-1	0.97	0.99	0.91	0.54	1.04E−6	12.29	10	Actin cross-link formation
Cluster 3: up-down regulation (22)									
gi|51592135	Cofilin-1	1.58	0.55	1.00	1.22	3.39E−8	43.98	11	Regulates actin cytoskeleton dynamics
gi|90200404	Triosephosphate isomerase 1	1.26	0.56	0.86	0.84	3.02E−7	17.34	5	Triosephosphate isomerase activity
gi|350584416	Parathymosin	1.29	0.91	0.65	0.95	4.36E−7	22.55	3	Mediate immune function
gi|335309827	Nuclear autoantigenic sperm protein	2.07	2.27	0.96	0.69	5.38E−9	7.71	4	Required for DNA replication
gi|335284315	RNA-binding protein FUS isoform 2	1.27	0.95	0.47	0.68	1.45E−7	4.44	2	mRNA splicing, via spliceosome
gi|350579350	Stomatin-like protein 2	0.87	1.43	1.09	0.43	6.82E−8	7.93	3	T cell receptor signaling pathway

Table 1 continued

Accession	Protein name	Ratio				P value	% Cov (95%)	Peptides (95 %)	Function
		12 hpi	24 hpi	36 hpi	48 hpi				
gi|350594172	Brain acid soluble protein 1	1.45	0.58	0.24	0.90	2.97E−8	32.02	5	Glomerular visceral epithelial cell differentiation
gi|335295652	Laminin subunit beta-1	1.64	0.89	0.67	0.85	1.75E−5	3.47	4	Cell migration
gi|346644699	Protein SET	1.36	0.93	2.03	0.46	1.05E−8	15.16	3	Involved in apoptosis, transcription, nucleosome assembly and histone chaperoning
gi|345199274	Glutaredoxin 3	1.33	0.82	2.38	0.65	5.65E−9	14.37	4	Protein disulfide oxidoreductase activity
gi|350591320	26S proteasome non-ATPase regulatory subunit 6	1.25	2.33	1.69	0.63	7.88E−9	7.35	4	Transcription coactivator activity
gi|162951821	Heterogeneous nuclear ribonucleoprotein A/B	1.24	1.33	0.67	1.24	2.47E−7	13.25	5	Binds single-stranded RNA
gi|346716324	Myosin regulatory light chain 2 protein isoform 2	1.54	0.69	1.03	0.86	1.14E−7	17.44	3	Cardiac myofibril assembly
gi|311249564	Heterogeneous nuclear ribonucleoprotein H	1.85	1.20	1.12	0.10	7.61E−9	15.81	7	Regulation of RNA splicing
gi|311247963	Apoptosis inhibitor 5 isoform 1	1.04	1.63	0.18	0.53	1.31E−8	4.20	2	Apoptosis
gi|350591535	Hypothetical protein LOC100522278	1.46	0.79	0.88	0.67	1.31E−7	7.92	2	None
gi|83921635	FKBP1A	1.47	0.77	0.62	1.09	1.03E−7	25.00	3	Beta-amyloid formation
gi|75069665	ADP-ribosylation factor-like protein 3	0.75	1.74	1.28	0.69	3.50E−8	14.29	2	Cilium morphogenesis
gi|48675927	Tropomyosin alpha-3 chain	2.19	0.70	0.90	1.04	1.03E−8	43.55	21	Binds to actin filaments
gi|350595802	SH3 domain-binding glutamic acid-rich-like protein	1.04	1.05	1.38	0.48	1.07E−7	18.97	2	SH3/SH2 adaptor activity
gi|194034833	Microfibrillar-associated protein 1	0.91	1.41	0.53	0.79	1.12E−7	7.06	2	Extracellular matrix organization
gi|311250943	28 kDa heat- and acid-stable phosphoprotein	1.18	1.29	1.46	0.62	1.18E−7	19.78	2	Enhances PDGFA-stimulated cell growth in fibroblasts
Cluster 4: down-up regulation (43)									
gi|40836021	Vimentin	0.97	0.57	0.55	1.58	3.85E−8	70.17	106	Class-III intermediate filaments
gi|28948618	Annexin A1	0.34	1.22	1.64	2.91	1.59E−9	43.93	26	Calcium/phospholipid-binding protein
gi|335291884	Histone H2B type 1	0.69	1.21	1.41	1.00	1.29E−7	57.94	23	Nucleosome assembly
gi|350578257	Heterogeneous nuclear ribonucleoprotein Q isoform 1	0.75	1.25	0.69	3.70	5.06E−10	17.17	9	mRNA processing
gi|335284210	HSP 27	0.74	0.99	1.49	1.26	1.94E−7	28.25	12	Stress resistance and actin organization
gi|350580027	Elongation factor 1-gamma	0.53	0.85	1.14	1.28	1.70E−7	17.85	7	Translation elongation factor activity
gi|194043605	GTP-binding nuclear protein Ran	0.59	1.31	0.99	2.19	9.64E−9	19.91	5	GTP-binding protein involved in nucleocytoplasmic transport
gi|9857227	Ribophorin I	0.39	0.74	1.49	0.88	4.69E−8	6.25	3	Glycotransferase activity
gi|311245228	Serpin B5	0.44	1.06	1.60	0.95	4.06E−8	10.67	3	Tumor suppressor
gi|350591497	ras-related protein Rab-7a	1.13	0.65	1.41	1.13	2.09E−7	20.09	3	Key regulator in endolysosomal trafficking

Table 1 continued

Accession	Protein name	Ratio				P value	% Cov (95%)	Peptides (95 %)	Function
		12 hpi	24 hpi	36 hpi	48 hpi				
gi|255683404	Isocitrate dehydrogenase	**0.48**	**1.33**	1.24	0.99	9.83E−8	7.52	3	NADPH regeneration
gi|343887407	Thiopurine S-methyltransferase	**0.68**	**0.56**	**1.72**	**1.60**	1.56E−8	22.04	4	Nucleobase-containing compound metabolic process
gi|335281298	Tubulin beta-2C chain	0.87	**0.65**	**1.43**	0.79	1.51E−7	24.27	17	Structural constituent of cytoskeleton
gi|8745552	Voltage-dependent anion channel 1	**0.62**	**1.69**	1.21	1.08	5.55E−8	25.44	6	Voltage-gated anion channel activity
gi|304365428	Protein disulfide-isomerase A3	1.11	**0.54**	**1.53**	1.11	7.62E−8	30.30	18	Signal transduction
gi|8745554	Voltage-dependent anion channel 2	**0.72**	**0.65**	**1.27**	**1.42**	9.28E−8	21.43	7	Voltage-gated anion channel activity
gi|194034450	Nidogen-2	**0.30**	**1.69**	1.18	1.03	1.91E−8	7.66	8	Cell–matrix adhesion
gi|75056558	Ras-related protein Rab-11A	**0.41**	**0.69**	**2.13**	**1.69**	4.84E−9	15.74	4	Melanosome transport
gi|346986294	Uncharacterized protein LOC100155717 isoform 2	**0.46**	**0.64**	**1.45**	**1.87**	1.04E−8	19.72	4	Peroxiredoxin (PRX)-like 2 family
gi|311245734	Hypothetical protein LOC100038023	1.00	**0.69**	1.18	**2.17**	6.97E−9	14.06	4	mTOR signaling pathway
gi|47522630	Aspartate aminotransferase	**0.61**	1.21	1.06	**1.85**	3.01E−8	11.63	6	Aspartate biosynthetic process
gi|346227216	Ribosomal protein L15	0.95	**0.74**	**1.39**	**2.09**	2.92E−8	7.84	2	Translational elongation
gi|311248936	Phenylalanyl-tRNA synthetase alpha chain	**0.50**	**0.35**	0.91	**1.38**	2.14E−8	4.33	2	tRNA aminoacylation for protein translation
gi|345441771	Aldolase C, fructose-bisphosphate	**0.61**	1.05	**1.43**	1.06	1.64E−7	8.24	2	Fructose metabolic process
gi|213958609	Glutamine:fructose-6-phosphate amidotransferase 1 variant 2	**0.34**	**4.13**	1.07	**5.11**	7.15E−11	6.58	3	Controls the flux of glucose into the hexosamine pathway
gi|281500757	Porcine Aldehyde Reductase In Ternary Complex With Inhibitor	**0.30**	**0.74**	1.11	**1.58**	2.37E−8	11.69	3	Alcohol dehydrogenase activity, zinc-dependent
gi|335284299	T-complex protein 1 subunit zeta	1.05	0.98	**0.71**	**1.56**	1.31E−7	12.62	5	ATP binding
gi|311247012	Epidermal growth factor receptor kinase substrate 8	1.14	**0.25**	**1.28**	0.89	4.81E−8	5.47	4	Rac protein signal transduction
gi|60394813	40S ribosomal protein S16	1.18	1.15	**0.65**	**4.61**	1.87E−10	13.01	2	rRNA processing
gi|346227222	Ribosomal protein L13a isoform 1	0.82	**0.52**	**1.96**	0.92	1.34E−8	10.78	2	Translation
gi|346421378	Serpin H1	0.95	**0.59**	0.99	**2.29**	6.74E−9	5.25	2	Binds specifically to collagen
gi|342349319	Calnexin	**0.14**	0.90	**2.33**	**1.50**	2.81E−9	5.40	3	Calcium ion binding
gi|346644805	Pinin	**0.63**	**1.57**	**1.33**	1.14	8.19E−8	1.23	2	Transcription regulation
gi|85681889	60S ribosomal protein L10	0.86	1.20	**0.60**	**1.89**	2.13E−8	6.08	3	Structural constituent of ribosome
gi|311252000	Fumarylacetoacetate hydrolase domain-containing protein 2	1.16	0.99	**0.52**	**2.83**	2.02E−9	3.51	2	Hydrolase activity
gi|54020966	Annexin A2	**0.74**	1.11	1.11	**2.61**	4.38E−9	37.76	20	Calcium-regulated membrane-binding protein
gi|350585373	Myosin-14	**0.72**	0.77	**2.25**	0.76	6.57E−9	10.17	8	ATP binding
gi|51870491	CDC37 cell division cycle 37 protein	**0.74**	1.12	**1.37**	1.06	4.61E−7	17.11	4	Cell division
gi|85792232	Eukaryotic translation initiation factor 4A isoform 1	**0.72**	**1.79**	**1.26**	0.89	4.13E−8	19.46	8	Cytokine-mediated signaling pathway

Table 1 continued

Accession	Protein name	Ratio				P value	% Cov (95%)	Peptides (95 %)	Function
		12 hpi	24 hpi	36 hpi	48 hpi				
gi|4033507	Annexin A4	0.71	1.45	1.54	1.09	1.01E−7	33.54	11	Calcium/phospholipid-binding protein
gi|343403779	Ribosomal protein L13	1.24	0.70	1.18	1.50	1.68E−7	7.11	2	Translational elongation
gi|45268967	40S ribosomal protein S28	1.17	0.74	1.51	0.77	1.16E−7	26.25	4	Translational elongation
gi|343432604	Ubiquitin-conjugating enzyme E2 variant 2	0.71	1.98	1.29	1.38	2.85E−8	21.38	2	Error-free post-replication DNA repair
Cluster 5: up-down-up regulation (6)									
gi|350588024	Heterogeneous nuclear ribonucleoprotein D0	1.09	1.37	0.74	1.27	3.53E−7	16.42	4	RNA catabolic process
gi|350586335	Nuclease-sensitive element-binding protein 1	1.27	0.77	0.95	2.17	1.39E−8	20.95	6	Mediates pre-mRNA alternative splicing regulation
gi|350585579	Alpha-enolase	1.39	0.61	2.15	1.18	1.26E−8	18.21	13	Magnesium ion binding
gi|85542092	60S ribosomal protein L6	1.60	0.59	1.43	2.21	1.04E−8	9.51	3	Translation
gi|194037373	Coatomer subunit zeta-1 isoform 1	3.10	0.59	3.56	1.11	4.58E−10	18.64	2	Intracellular protein transport
gi|350594189	Cadherin-10	1.60	1.38	0.63	1.46	5.83E−8	3.16	2	Calcium ion binding
Cluster 6:down-up-down regulation (11)									
gi|342672022	exportin-2	0.74	0.64	1.32	0.47	1.12E−7	3.60	4	cell proliferation
gi|350583346	ubiquitin associated protein 2-like isoform 3	0.57	0.94	3.31	0.56	3.86E−10	3.04	2	binding of sperm to zona pellucida
gi|335309813	coactosin-like protein	0.96	0.68	1.26	0.26	6.36E−8	12.50	2	Binds to F-actin in a calcium-independent manner
gi|350578507	asparaginyl-tRNA synthetase	0.94	0.41	1.63	0.73	2.92E−8	6.80	4	tRNA aminoacylation for protein translation
gi|350596594	malate dehydrogenase	0.56	0.57	1.28	0.53	1.18E−7	20.76	7	L-malate dehydrogenase activity
gi|60389430	m7GpppX diphosphatase	0.56	1.43	0.82	0.65	8.83E−8	10.09	2	cellular response to menadione
gi|350529411	proteasome (prosome, macropain) 26S subunit, ATPase, 2	0.51	2.73	2.91	0.61	7.12E−10	13.63	5	enzyme regulator activity
gi|51317314	Histone H4	0.07	1.94	0.28	1.19	3.75E−9	50.49	7	Core component of nucleosome
gi|194044626	14-3-3 protein beta/alpha isoform 1	1.04	0.69	1.54	0.65	7.19E−8	32.52	8	Ras protein signal transduction
gi|350578528	peptidyl-prolyl cis-trans isomerase B	0.72	0.62	1.34	0.29	5.62E−8	23.20	5	PPIases accelerate the folding of proteins
gi|335282599	interleukin enhancer-binding factor 3	0.30	0.70	2.83	0.58	1.13E−9	11.95	6	Transcription regulation
Cluster 7:up-down-up-down regulation (1)									
gi|335290365	45 kDa calcium-binding protein	1.39	0.59	1.45	0.48	2.99E−8	4.48	2	calcium ion binding
Cluster 8: down-up-down-up regulation (1)									
gi|350594669	ribosome-binding protein 1	0.69	1.64	0.63	1.92	1.11E−8	4.25	5	rRNA processing

The 196 unique proteins identified with 95% confidence (corresponding to a protein score cutoff >1.3), were clustered based on similar trends of differential 489 expression over times. % Cov (95) means percent coverage (95%). The proteins were considered to show a significant upward or downward trend if their expression 490 ratios relative to the mock control group at the same time post infection were >1.25 or <0.75, respectively. One-way analysis of variance (ANOVA) and LSD analysis 491 (SPSS 18.0) were used in this statistical test. Differences between groups through the time course were considered statistically significant for P values < 0.05
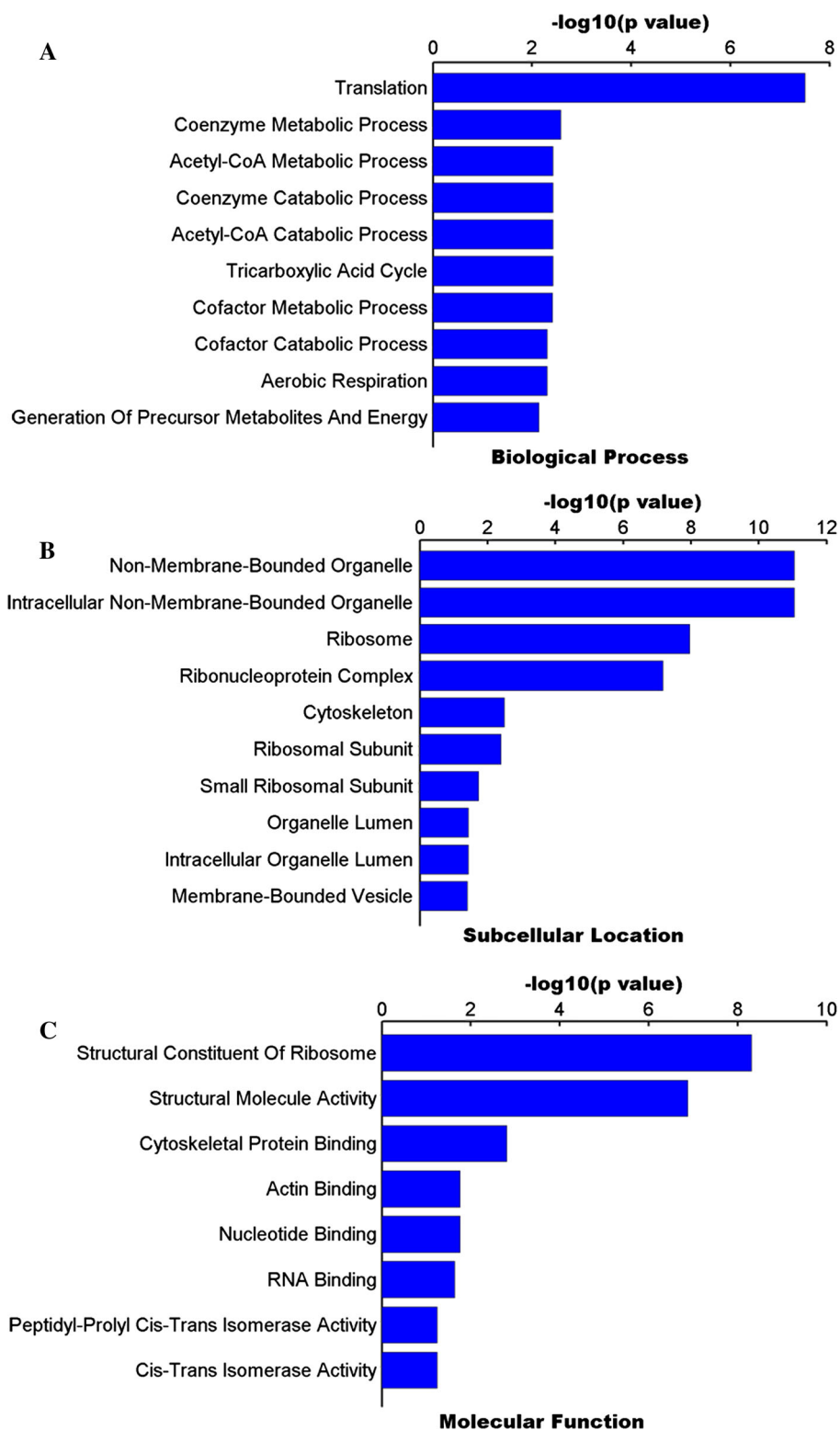
Validation of changes in protein levels via Western blot

To validate the differentially expressed proteins identified using the iTRAQ labeled LC–MS/MS system, vimentin, Annexin I, Hsp90, and Rab-11A were selected for Western

blot analysis. Equal amounts of cell lysate protein from PCV2-infected PK-15 and virus-free cells were tested with antibodies against vimentin, AnnexinI, Hsp90, and Rab-11A, respectively. As shown in Fig. 6, the Hsp90 was up-regulated at 96 hpi. In addition, the expression of vimentin,
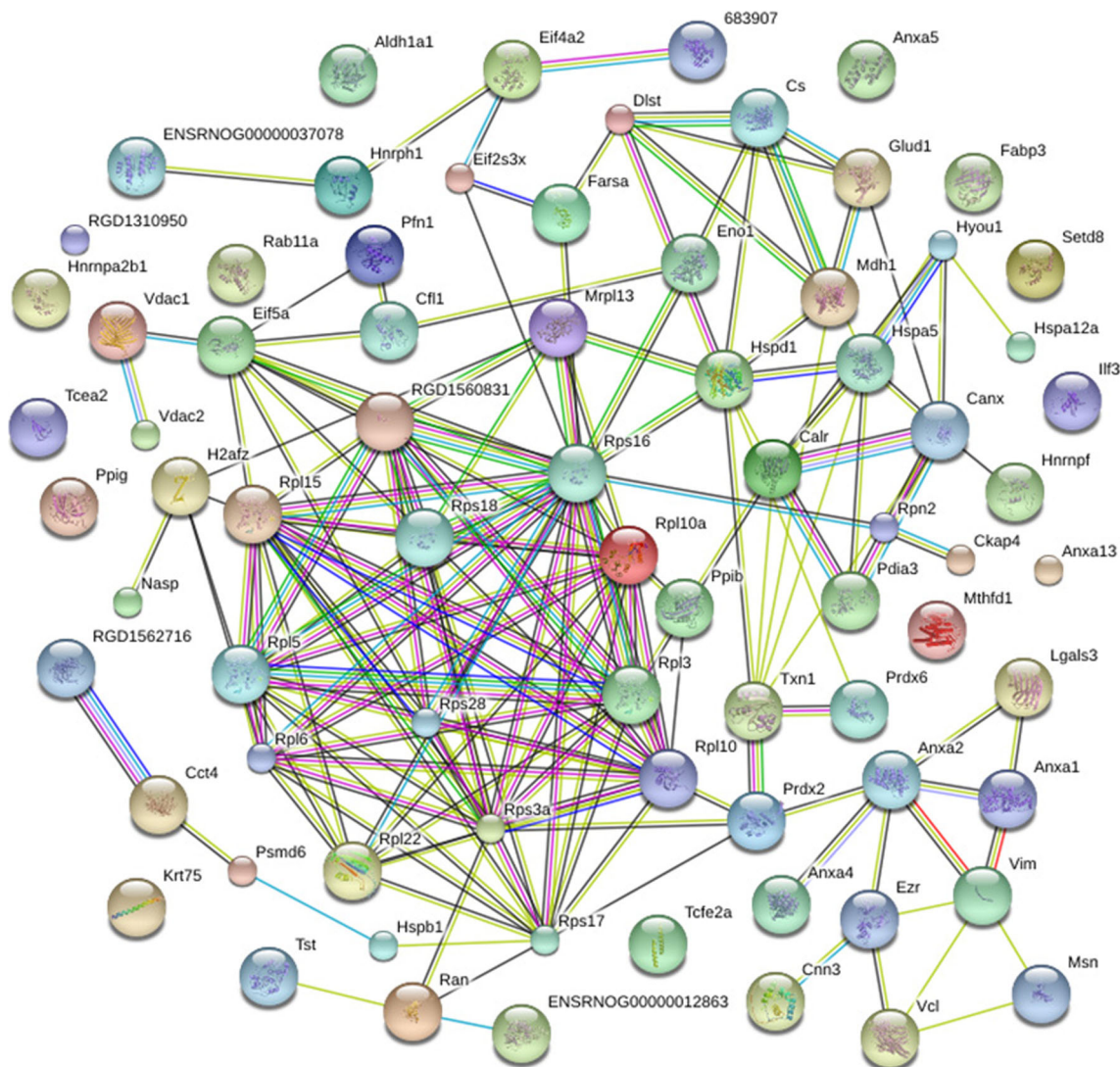
Fig. 5 Protein–protein interaction network analyzed via STRING software. An edge was drawn with up to seven different colored lines representing the existence of seven lines of evidence used in predicting associations. A *red line* indicates the presence of fusion evidence, a *green line* indicates neighborhood evidence, a *blue line* indicates co-occurrence evidence, a *purple line* indicates experimental evidence, a *yellow line* indicates text mining evidence, a *light blue line* indicates database evidence, and a *black line* indicates co-expression evidence (Color figure online)

AnnexinI, and Rab-11A showed down-regulation in the prophase of infection, and then, they up-regulated later. The ratios of the four representative proteins between infected and uninfected cells were consistent with those obtained from iTRAQ-coupled 2D LC–MS/MS analysis. Protein spot levels were determined using ImageJ quantification software.

Discussion and conclusions

Upon virus infection, cellular environments are modified to eliminate the invading virus by host antiviral responses or to favor virus replication by viral evasion strategies. The changes of host gene production in virus-infected cells have been largely studied to elucidate pathogenic mechanism associated with such alterations. However, very limited information is currently available for cellular protein productions regulated after exposed to individual viral components. To further elucidate the molecular mechanisms involved in PCV2 infection of host cells, we screened the differentially expressed proteins associated with PK-15 cells infected with the virus using comparative proteomics. Several earlier studies have analyzed the interplay between PCV2 and host cells using proteomics analysis, which includes interactions of PCV2 and PK-15
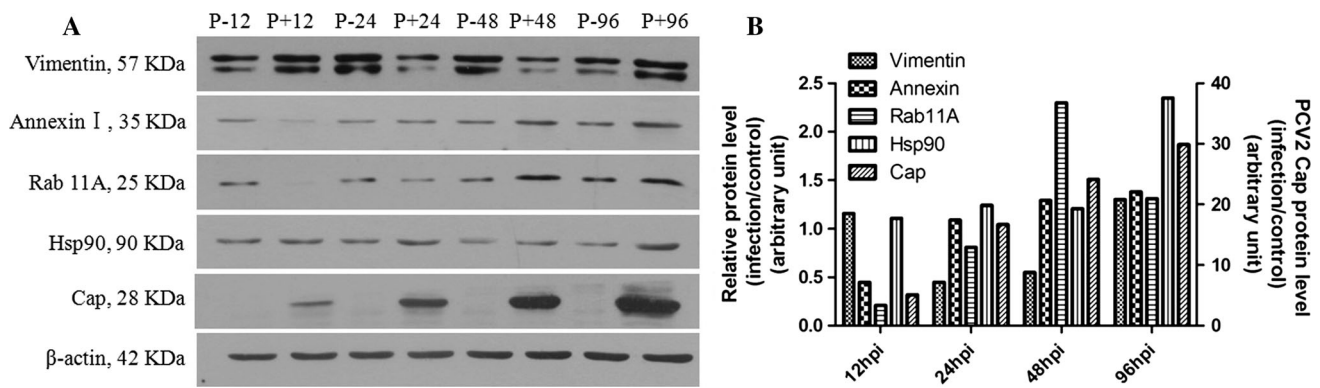
Fig. 6 Confirmation of four differentially expressed proteins (vimentin, Annexin I, Rab11A, and Hsp90) and viral Cap protein in PCV2-infected PK-15 cells using Western blot analysis (**a**). The levels of relative proteins were quantified with immunoblot scanning and normalized to the amount of β-actin (**b**)

cells [15, 16], porcine alveolar macrophages (PAMs) [17, 18], and inguinal lymph nodes of piglets inoculated with PCV2 [14]. In order to determine further virus–host interactions and the processes leading to disease onset, a high-throughput quantitative proteomic approach, iTRAQ was utilized to investigate the differential proteomes of a highly permissive PK-15 clone cells in response to PCV2 infection. The results indicated that a total of 196 proteins displayed significantly altered expression at different time points post-infection. Four of these proteins were confirmed to be regulated in PCV2-infected PK-15 cells using immunoblotting as an independent analytical method. It provided critical clues for further analysis of PCV2 pathogenesis.

Proteomics is a novel methodology employed to detect the components of cellular protein interactions as well as host cellular pathophysiological processes that occur during virus infection [25, 26]. iTRAQ, combined with LC and tandem MS analysis, is emerging as a powerful technology in the search for disease-specific targets. This procedure is ideally suited to our study, since it allows the comparison of four time points after infection and four corresponding controls. Compared with mock infection, PCV2 did not induce visible cytopathic effects. Furthermore, the full cell monolayer appeared in PCV2-infected cells. Both IFA and Western blot results disclosed that PCV2 replicates in PK-15 cells. Differentially expressed proteins are involved in cytoskeleton organization, macromolecular biosynthesis, signal transduction, stress response, ubiquitin–proteasome pathway (UPP), and metabolic enzymes (Table 1). Our data aid in the understanding of the pathogenesis of PCV2 infection. In our previous quantitative proteomics study, we identified that Hsp70 was up-regulated in PCV2-infected PAMs [18]. Then, we firstly found that Hsp70 could positively regulate PCV2 replication in a continuous porcine monocytic cell line 3D4/31 [27]. It can be seen that

the results of proteomics study should be useful to elucidate the mechanism of replication of PCV2 in the future.

The host cytoskeletal network participates in the transport of viral components in the cell, particularly during the stages of the entry and exit of the virus [28]. Our data strongly indicate an important role for cytoskeletal proteins in PCV2 infection in PK-15 cells. The identified microfilament-associated and microtubule-associated proteins, i.e., annexin A2 and beta 5-tubulin, were up-regulated (Table 1), whereas the microtubule-associated protein 4, alpha-actin, and keratin 8 were down-regulated in the process of infection (Table 1). The existing evidence suggests that actin can regulate gene transcription in virus-induced signaling. The mRNA-binding activity of actin is important for the anchoring, transporting, and topological positioning of mRNAs [29]. With regard to β-tubulin, there are several reports showing that viruses may require microtubule components for RNA synthesis [30]. α-tubulin was identified as being overexpressed when it interacts with Rep of PCV2 through colocalization and coimmunoprecipitation analyses [15]. Changes in β-tubulin and vimentin levels have been detected in SARS-CoV22 and infectious bursal disease virus (IBDV) [26, 31]. However, Fan et al. [16.] indicated that β-tubulin level was down-regulated in infected PK-15 cells and speculated that the vimentin and β-tubulin networks collapse and disperse in host cells, leading to an unstable cytoskeletal structure and release of viral particles from the infected cells. The roles of these cytoskeletal proteins in PK15 cells after PCV2 infection should be further investigated.

Heat shock proteins (HSPs) are a class of multifunctional proteins that maintain cell stability when cells are exposed to elevated temperatures, pathogens, and/or other environmental stresses [32]. Activation of the heat shock response might be a specific virus function that ensures proper synthesis of viral proteins and virions; thus, stress

proteins may be important for virus replication [33]. Mammalian cells have developed response networks which detect and control diverse forms of stress. One of these responses, known as heat shock response, is a universal mechanism necessary for cell survival under a variety of unfavorable conditions like virus infections [34]. In the present study, the up-regulation of Hsp90, Hsp70, and Hsp60 was identified in the PCV2-infected PK-15 cells (Table 1). Hsp60 is a mitochondrial chaperonin that is typically responsible for the transportation and refolding of proteins from the cytoplasm into the mitochondrial matrix, and it was reported that Hsp60 folds 30 % of the cytoplasmic proteins under heat stress [35]. One study reported that Hsp60 can directly activate leukocytes, epithelial cells, and fibroblasts to secrete proinflammatory cytokines such as TNF and interleukins, which participate in the process of T cell-mediated immunity [36]. It has been reported that HSPs inhibit the replication of IV and a variety of RNA viruses [37]. Inhibition of the expression of Hsc70 blocks the nuclear export of the IV M1 and NP proteins and thereby inhibits the production of the progeny virus [37]. Previously, we demonstrated that Hsp70 has a positive regulatory effect on PCV2 infection cycle, based on proteomics results on PCV2-infected PAMs [27]. Hsp90 has a very important function in the folding of cell regulatory proteins and the refolding of stress-denatured polypeptides [38–40]. Prior research has also shown that Hsp90 is involved in the assembly and nuclear export process of IV RNPs [41]. A previous report showed that an initial increase in Hsp90 expression at 12 h after infection suggests a cellular response to hMPV-induced ER stress initiated by an increase in unfolded or misfolded proteins [42]. Recently, an association between Hsp90 protein complex and lamin A/C has been observed after oxidative stress [43]. Also, in our PCV2-infected PK-15 cells, we observe an increase in Hsp90 and lamin subunit beta. Here, the increased information should be helpful to study on the molecular mechanisms underlying host–PCV2 interactions.

Several signal transduction-associated proteins were identified to be differentially expressed in the PCV2-infected cells. The 14-3-3 protein family is known to be involved in the regulation of several signal transduction pathways including those regulating the cell cycle, apoptosis, cytoskeletal remodeling, transcription, and stress responses [44]. A prior study reported that the 14-3-3 protein interacts with the HCV core protein to activate kinase Raf-1 [45], and the identified interaction of the 14-3-3 protein with Vpr has a functional significance for cell cycle regulation in HIV-1 infection [46]. In our study, the expression of 14-3-3 protein in PCV2-infected PK-15 cells was down-regulated. This occurrence may be due to the cellular physiology dysfunction of PK-15 cells. Further

work is clearly necessary to examine the function of 14-3-3 protein in PCV2-infected tissues.

Ubiquitin–proteasome pathway (UPP), a major intracellular protein degradation pathway, has recently been implicated in viral infections, including avoidance of host immune surveillance, viral maturation, viral progeny release, efficient viral replication, and reactivation of virus from latency [47]. Some viruses have been reported to evolve different strategies to utilize the UPP for beneficial reasons, including the indication that ubiquitin–proteasome system is required for avoidance of host immune surveillance during HIV-1 and is necessary for transcriptional regulation of the DNA virus, herpes simplex virus (HSV) [48, 49]. Mumps virus and simian virus inhibit JAK/STAT signaling pathway through proteasome degradation of the cellular STAT protein to escape the interferon-initiated antiviral responses [50]. In this study, PCV2 infection induced expression of the ubiquitin-conjugating enzyme E2, proteasome 26S subunit, and ubiquitin-associated protein 2. Therefore, their change in abundance levels may indicate to an important pathway affected by PCV2 replication. Whether PCV2 takes the similar or different strategy during infection has not been elucidated and deserves further investigation.

In summary, in this study, an iTRAQ proteomics approach was adopted to probe differentially expressed proteins in PCV2-infected PK-15 cells. Using unambiguous methods, we identified 196 cellular proteins that were significantly altered following PCV2 infection. The abundance of differentially expressed proteins should aid in elucidating molecular mechanisms associated with interactions between PCV2 and target cells. However, the proteomics results were preliminary data, which needed to be further elaborated and analyzed for understanding the roles of these proteins in PCV2 infection.

References

1. I. Tischer, H. Gelderblom, W. Vettermann, M.A. Koch, Nature **295**, 64–66 (1982)
2. Q. Liu, S.K. Tikoo, L.A. Babiuk, Virology **285**, 91–99 (2001)
3. P. Nawagitgul, I. Morozov, S.R. Bolin, P.A. Harms, S.D. Sorden, P.S. Paul, J gen virol **81**, 2281–2287 (2000)
4. G. Allan, B. Meehan, D. Todd, S. Kennedy, F. McNeilly, J. Ellis, E.G. Clark, J. Harding, E. Espuna, A. Botner, C. Charreyre, Vet. Rec. **142**, 467–468 (1998)

5. J. Ellis, L. Hassard, E. Clark, J. Harding, G. Allan, P. Willson, J. Strokappe, K. Martin, F. McNeilly, B. Meehan, D. Todd, D. Haines, Canadi vet j La rev vet canadi **39**, 44–51 (1998)

6. T. Shibahara, K. Sato, Y. Ishikawa, K. Kadota, J vet med sci/ Jpn Soc Vet Sci **62**, 1125–1131 (2000)

7. G. Lee, D. Han, J.Y. Song, Y.S. Lee, K.S. Kang, S. Yoon, J gen virol **91**, 2585–2591 (2010)

8. S. Krakowka, J.A. Ellis, B. Meehan, S. Kennedy, F. McNeilly, G. Allan, Vet. Pathol. **37**, 254–263 (2000)

9. S.R. Bolin, W.C. Stoffregen, G.P. Nayar, A.L. Hamel, J vet diagn investig **13**, 185–194 (2001)

10. N. Thanthrige-Don, M.F. Abdul-Careem, L.A. Shack, S.C. Burgess, S. Sharif, Virol **390**, 356–367 (2009)

11. Y.H. Lai, Z.C. Li, L.L. Chen, Z. Dai, X.Y. Zou, J proteomics **75**, 2500–2513 (2012)

12. X. Feng, J. Zhang, W.N. Chen, C.B. Ching, J proteomics **74**, 567–576 (2011)

13. R. Ralhan, L.V. Desouza, A. Matta, S. Chandra Tripathi, S. Ghanny, S. Datta Gupta, S. Bahadur, Mol & cell proteomics **7**, 1162–1173 (2008)

14. M. Ramirez-Boo, E. Nunez, I. Jorge, P. Navarro, L.T. Fernandes, J. Segales, J.J. Garrido, J. Vazquez, A. Moreno, Proteomics **11**, 3452–3469 (2011)

15. X. Zhang, J. Zhou, Y. Wu, X. Zheng, G. Ma, Z. Wang, Y. Jin, J. He, Y. Yan, J. Proteome Res. **8**, 5111–5119 (2009)

16. H.Y. Fan, Y. Ye, Y.W. Luo, T.Z. Tong, G.R. Yan, M. Liao, J. Proteome Res. **11**, 995–1008 (2012)

17. S. Cheng, M. Zhang, W. Li, Y. Wang, Y. Liu, Q. He, J proteomics **75**, 3258–3269 (2012)

18. J. Liu, J. Bai, Q. Lu, L. Zhang, Z. Jiang, J.J. Michal, Q. He, P. Jiang, J proteomics **79**, 72–86 (2013)

19. M.B. Eisen, P.T. Spellman, P.O. Brown, D. Botstein, Proc. Natl. Acad. Sci. U.S.A. **95**, 14863–14868 (1998)

20. A.J. Saldanha, Bioinformatics **20**, 3246–3248 (2004)

21. G. Dennis, B.T. Sherman, D.A. Hosack, J. Yang, W. Gao, H.C. Lane, R.A. Lempicki, Genome biol **4**, P3 (2003)

22. D.W. Huang, B.T. Sherman, R.A. Lempicki, Nat. Protoc. **4**, 44–57 (2009)

23. Z. Zhang, L. Zhang, Y. Hua, X. Jia, J. Li, S. Hu, X. Peng, P. Yang, M. Sun, F. Ma, Z. Cai, BMC Cancer **10**, 206 (2010)

24. V. Gerke, C.E. Creutz, S.E. Moss, Nat. Rev. Mol. Cell Biol. **6**, 449–461 (2005)

25. K.L. Maxwell, L. Frappier, Microbiol. Mol. Biol. Rev. **71**, 398–411 (2007)

26. X. Zheng, L. Hong, L. Shi, J. Guo, Z. Sun, J. Zhou, Mol & cell proteomics **7**, 612–625 (2008)

27. J. Liu, J. Bai, L. Zhang, Z. Jiang, X. Wang, Y. Li, P. Jiang, Virology **447**, 52–62 (2013)

28. K. Radtke, K. Dohner, B. Sodeik, Cell. Microbiol. **8**, 387–400 (2006)

29. F. Miralles, N. Visa, Curr. Opin. Cell Biol. **18**, 261–266 (2006)

30. P.O. Chongsatja, A. Bourchookarn, C.F. Lo, V. Thongboonkerd, C. Krittanai, Proteomics **7**, 3592–3601 (2007)

31. X.S. Jiang, L.Y. Tang, J. Dai, H. Zhou, S.J. Li, Q.C. Xia, J.R. Wu, R. Zeng, Mol & cell proteomics **4**, 902–913 (2005)

32. D.R. Ciocca, S. Oesterreich, G.C. Chamness, W.L. McGuire, S.A. Fuqua, J. Natl Cancer Inst. **85**, 1558–1570 (1993)

33. J.B. Glotzer, M. Saltik, S. Chiocca, A.I. Michou, P. Moseley, M. Cotten, Nature **407**, 207–211 (2000)

34. M.G. Santoro, Biochem. Pharmacol. **59**, 55–63 (2000)

35. J. Zhu, W. Zou, G. Jia, H. Zhou, Y. Hu, M. Peng, H. Chen, M. Jin, J proteomics **75**, 1732–1741 (2012)

36. R.M. Vabulas, P. Ahmad-Nejad, C. da Costa, T. Miethke, C.J. Kirschning, H. Hacker, H. Wagner, J. Biol. Chem. **276**, 31332–31339 (2001)

37. K. Watanabe, T. Fuse, I. Asano, F. Tsukahara, Y. Maru, K. Nagata, K. Kitazato, N. Kobayashi, FEBS Lett. **580**, 5785–5790 (2006)

38. B. Chen, W.H. Piel, L. Gui, E. Bruford, A. Monteiro, Genomics **86**, 627–637 (2005)

39. P. Csermely, T. Schnaider, C. Soti, Z. Prohaszka, G. Nardai, Pharmacol. Ther. **79**, 129–168 (1998)

40. W.M. Obermann, H. Sondermann, A.A. Russo, N.P. Pavletich, F.U. Hartl, J cell biol **143**, 901–910 (1998)

41. F. Momose, T. Naito, K. Yano, S. Sugimoto, Y. Morikawa, K. Nagata, J. Biol. Chem. **277**, 45306–45314 (2002)

42. A. van Diepen, H.K. Brand, I. Sama, L.H. Lambooy, L.P. van den Heuvel, L. van der Well, M. Huynen, A.D. Osterhaus, A.C. Andeweg, P.W. Hermans, J proteomics **73**, 1680–1693 (2010)

43. M. Nakamura, H. Morisawa, S. Imajoh-Ohmi, C. Takamura, H. Fukuda, T. Toda, Exp. Gerontol. **44**, 375–382 (2009)

44. D. Thomas, M. Guthridge, J. Woodcock, A. Lopez, Curr. Top. Dev. Biol. **67**, 285–303 (2005)

45. H. Aoki, J. Hayashi, M. Moriyama, Y. Arakawa, O. Hino, J. Virol. **74**, 1736–1741 (2000)

46. T. Kino, A. Gragerov, A. Valentin, M. Tsopanomihalou, G. Ilyina-Gragerova, R. Erwin-Cohen, G.P. Chrousos, G.N. Pavlakis, J. Virol. **79**, 2780–2787 (2005)

47. G. Gao, H. Luo, Can. J. Physiol. Pharmacol. **84**, 5–14 (2006)

48. U. Schubert, L.C. Anton, I. Bacik, J.H. Cox, S. Bour, J.R. Bennink, M. Orlowski, K. Strebel, J.W. Yewdell, J. Virol. **72**, 2280–2288 (1998)

49. Q. Zhu, J. Yao, G. Wani, J. Chen, Q.E. Wang, A.A. Wani, FEBS Lett. **556**, 19–25 (2004)

50. B. Gotoh, T. Komatsu, K. Takeuchi, J. Yokoo, Rev. Med. Virol. **12**, 337–357 (2002)